Grouting of cohesionless soils by means of colloidal nanosilica

Case Studies in Construction Materials 15 (2021) e00577

Contents lists available at ScienceDirect

Case Studies in Construction Materials

journal homepage: www.elsevier.com/locate/cscm

Case study

Grouting of cohesionless soils by means of colloidal nanosilica

Carmine Todaro

DIATI – Politecnico di Torino, Corso Duca degli Abruzzi 24, 10129, Torino, Italy

ARTICLE INFO

Keywords:
Grouting
Ground improvement
Colloidal nanosilica
Nanosilica accelerators
UCS
Gelling time
Dynamic viscosity
Tensile strength
Shear strength

ABSTRACT

Colloidal nanosilica is an innovative grouting material, currently used in tunnelling applications for grouting fine cohesionless soils when environmental limits prevent the application of other solutions. Despite a large number of applications, knowledge of operational parameters for grouting such as gelling time and dynamic viscosity is very limited. Furthermore, the influence of the type of nanosilica (in terms of SiO_2 concentration) and accelerators on the achievable mechanical performance of injected soils has never been investigated. In this work, a laboratory test campaign based on two commercial colloidal nanosilica and two accelerators was conducted. Once the operational parameters had been investigated, four different soils have been grouted and, after curing, mechanically tested. The results, in terms of gelling time and viscosity order of magnitude, are crucial for the correct functioning of a grouting. Furthermore, the results of the uniaxial compression tests, the indirect tensile tests and the direct shear tests have shed light on the potential of colloidal nanosilica and on the differences between the chemicals.

1. Introduction

In the context of an urban area, shallow tunnels are often demanded for transport or hydraulic reasons. In the case of cohesionless soils, often the tunnel construction constitutes for buildings a concrete risk of damage or can cause collapse directly (by deformation in the ground) or indirectly (by lowering of groundwater), which cannot be neglected in the design phase [1–4]. In these cases, different stabilization technologies can be applied even if the main used are undoubtedly the jet grouting and the grouting. Pertaining to the first one, the method consists of loosening the soil with high-velocity jet in a predrilled borehole and mixing it with cement in order to create rigid bodies with a certain depth to the ground surface [5,6]. Jet grouting can be used both in sands or clay [7,8]. Concerning the grouting, it is a consolidation technique based on the injection of specific material into sands or in rock fractures with a certain pressure [9,10]. Irrespective of the type of consolidation, two main effect can be achieved by applying the grouting technique on cohesionless soils: reduction of permeability (in some cases reaching an almost waterproof medium) and increased mechanical performance of the grouted medium [11,12]. Due to these results, face instability, surface settlements, and water inflows can be easily controlled by previously applying an effective grouting operation [2].

Focusing on the grouting teqnuique, to predict the feasibility of a grouting operation, different acceptance criteria have been introduced in the last decades. Camberfort [13] introduced an acceptance criterion based on the permeability of the soil intended for injection, while other authors observed that the key to successful grouting is the significant diameters of both the grouting material and soil intended for injection [14,15]. Bodocsi and Bowers [16] identified the viscosity of the grouting material as the key parameter for a successful injection operation, while recently, Akbulut and Saglamer [17] introduced an equation based on both parameters of the ground (in particular significant diameters) and grouting material parameters. According to these researches, chemical firms dedicated

E-mail address: carmine.todaro@polito.it.

https://doi.org/10.1016/j.cscm.2021.e00577
Received 29 January 2021; Received in revised form 21 March 2021; Accepted 13 May 2021
Available online 15 May 2021

to grouting products run research paths aimed at optimizing the interaction between the grouting material and soils to be grouted, marketing innovative products that are able to successfully permeate a broad range of grain size distributions. From mortar made of standard Portland cement, the technology moved towards the use of microfine cement [18], whereupon colloidal nanosilica was used firstly mixed with microfine cement [19–21] and secondly as standalone grouting material. Fig. 1 summarized graphically this evolution concept: different grouting material are reported, scaled in function of a reference dimension of 0.01 mm. From right to left, according to a decreasing trend of grain size dimension, the high fineness of colloidal nanosilica is highlighted compared to other materials.

However, the choice of a suitable grouting material, besides the permeation potential linked to dimensions, is also a function of the final achievable mechanical performances of the final medium, according to the construction site requirements. While achievable performances are well-known for cement and microfine cement [18,22,23], information concerning colloidal nanosilica is more sporadic. It is used mainly in sands (even if some applications have been performed in fractured rocks, as discussed by Funehag and Gustafson [24]), and several authors have advanced the improvement of the mechanical performances reached after grouting. Yonekura and Miwa [25] and Persoff et al. [26] highlighted increases of the UCS, reaching an order of magnitude of hundreds of kilopascals. Chieregato et al. [27] introduced the dependence of the final UCS values of injected sands on the accelerator quality, reaching values higher than 1 MPa at 14 days of curing. Kakavand and Dabiri [28] successfully injected silty sands (with silt contents of 5, 10, and 15 % by weight) by using colloidal nanosilica. The authors highlighted the growth of the cohesion and friction angle in the injected material compared to the non-injected state in dry condition (3.4, 1.34, and 1.26 % for cohesion and 1.15, 1.23, and 1.17 % for the friction angle, respectively, for the three tested sands).

The literature analysis shows that the mechanical characterization of grouted sands performed by using colloidal nanosilica has been tackled but the results are not homogeneous. The different order of magnitude found for the UCS, for example, highlight a certain degree of lack that turns in difficulties, for grouting engineers, to understand if the usage of colloidal nanosilica could satisfy or not a certain technical specification. Anyway, the main recognized scientific gap is the complete absence of information concerning the kind of nanosilica used, consequently making it impossible to compare the results of different works. More in detail, for “colloidal nanosilica” are intended, all around the world, all water solution with different percentage of nanometric SiO_2. Consequently, all experimentations already published cannot be repeated being unknown the properties of the used colloidal nanosilica solution. Secondly, the available data are not useful for predicting a certain strength of soils after grouting, being the final mechanical results strongly affected by the used grouting material.

Furthermore, at the state of the art no references to colloidal nanosilica accelerator are available. As for the colloidal nanosilica, also for accelerators, the choice of products available on the market is wide. In addition, no information pertaining to how different accelerators influence the dynamic viscosity and the gel time (operative grouting parameters) and the final results in terms of strength are available.

In conclusion, the final gap recognizable in the scientific literature concerns the absence of a complete test campaign able to characterized mechanically a grouted soils obtained by using nanosilica and accelerator of known properties.

In the light of these scientific gaps, in this research two different colloidal nanosilica products and two different accelerators were considered. Preliminarily, the issues of the viscosity and gelling phenomenon were investigated for the purpose of providing the orders of magnitude of these parameters, which are crucial for the grouting feasibility and for the selection of more suitable injection equipment. Secondly, four sands have been taken as reference for the study. Hence, these sands were grouted with the colloidal nanosilica mixture, cured for pre-scheduled time spans and finally mechanically tested. Outcomes in terms of uniaxial compression strength (UCS), tensile strength, and the Mohr-Coulomb failure criteria envelope allowed a comparison between colloidal nanosilica mixtures, providing a reliable pattern of results that could be potentially useful for engineers involved in grouting.

2. Materials

2.1. Colloidal nanosilica

Colloidal nanosilica is a hydrophilic mineral mixture characterized by low viscosity. This mixture is composed of a water solution of

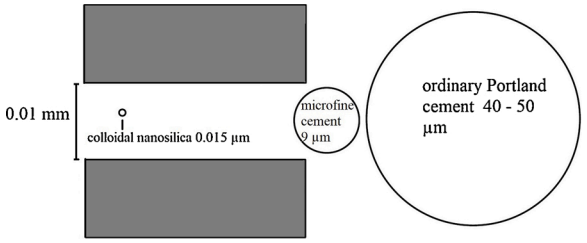

Fig. 1. Grain dimensions of standard Portland, microfine cement, silica fume, and colloidal nanosilica compared to a joint with an opening of 0.01 mm.

nanometric colloidal silica, and due to its chemical composition it is considered a harmless grouting material for both humans and environment [29]. The main advantage offered by colloidal nanosilica respect other kinds of non-cementitious grout is the non-toxicity, as hilighted by G.LazzaraS & Milioto [30] that reported the usage of nanosilica also in medicine and drug delivery.

The suspension particles are quartz (SiO_2) with atoms in a tetrahedral distribution (amorphous forms). The surface of the silica particles is negatively charged, and consequently the repulsion forces ensure stability of the mixture before grouting. The size of the particles ranges from 4 to 16 nm and consequently the fineness of the material is very high, with a value of specific surface ranging between 170 and 750 m^2/g. In order to create a suitable mass for grouting, the repulsive forces have to be reduced. This occurs by adding an accelerator which induces the formation of Si-O-Si bonds [27]. This phenomenon is called jellification, and the gel time (the time needed for the nanosilica–accelerator mixture to lose its fluidity) can be controlled by changing the ratio of colloidal nanosilica and accelerator.

In this research, two different commercial colloidal nanosilica products were considered. The choice to use two commercial products was taken in order to avoid potential operative mistakes during the preparation of the water solution. Furthermore, being products produced in chemical firms, the properties of content of SiO_2, particle size dimensions, surface, viscosity and density were certified on data sheets.

To streamline reading of the paper, colloidal nanosilica products A and B are hereinafter also referred to as “CNA” and “CNB”. The main properties of these products are summarized in Table 1.

CNA has a higher concentration of SiO_2 and a bigger particle size dimension than CNB. CNB is finer, with a fineness four time higher than CNA.

2.2. Colloidal nanosilica accelerators

Two different kinds of accelerators were used. Both products consist of NaCl solution, with percentages by weight of 10 and 25 % respectively. The choice of these commercial products was made firstly to save time and secondly to reduce the number of potential further variables due to the use of a “homemade product” (the commercial products were certified). It should be declared that there are no contraindications to creating and using NaCl solutions with different concentrations of salt. In the following, accelerators 1 and 2 refer to NaCl concentrations equal to 10 and 25 %, respectively, and to streamline reading of the paper, are hereinafter referred to as “acc1” and “acc2”.

2.3. Injected soils

Four different soils were used for this study. Grain size distributions were “artificial”, namely soils were prepared in the laboratory with the purpose to obtain a pattern of reference materials wider as possible, centered however on the area proper of sands. This choice was made in order to assess whether the shape of the grain size distribution could influence the final mechanical properties of the injected grout, working always in the field of sands (the more realistic for grouting performed with the colloidal nanosilica).

A fluvial sand characterised by 6% by weight of silt was the cornerstone, i.e. all prepared soils contained a fixed amount of this sand, equal to 50 % by weight. The completion of samples have been obtained by adding the further 50 % by weight of gravel 2–5 mm, sand 0.2 mm, crushed sand 0.5 mm and sand 0.6 mm respectively for obtaining soils A, B, C and D. After preparation of the soils, the hydraulic conductivity (k) was assessed according to ASTM D2434-19 [31] in order to verify the occurrence of the wanted differences between soils also from an hydraulic point of view. As expected, the prepared materials looked rather different at a visual checking and exhibited differences in terms of grain size distribution (d_{10}, d_{60}, uniformity coefficient – U), hydraulic conductivity and density. Table 2 shows pictures and the main properties of the soils used while Fig. 2 depicts the grain size distributions. The information pertaining to the fluvial sand is reported only for completeness, as this material alone was not part of the grouting test.

Considering the first significant diameter d_{10}, marginal differences can be recognized between all soils, with a numerical value close to 0.1 with the exception of soil D (doubled value). As concerns the d_{60}, soils B, C and D exhibited a growing trend (from about 0.3 to 0.5) while soil A shows a marked bigger value equal to 3. Consequently, also U for soil A is of a bigger order of magnitude respect other soils, sign of a clear coarse nature. Pertaining to the hydraulic conductivity, it is evident that successful injection could be more problematic in soils B and D, while soil A exhibited the highest value, underscoring again its coarser nature. Pertaining values of density, very similar values have been obtained for soils B and C (close to 1.6 kg/L) and A and D (close to 1.7 kg/L). In conclusion, it can be stated that differences between prepared soils were appreciable, consequently samples were considered suitable for the subsequent investigation steps.

Table 1
Used colloidal nanosilica: main properties.

Properties	Unit of measure	CNA	CNB
Content of SiO_2	(%)	40	15
Particle size	(nm)	16	4
Specific surface	(m^2/g)	170	750
Viscosity (at 20 °C)	(mPa·s)	5	<10
Density (at 20 °C)	(kg/L)	1.25	1.1

Table 2
Photographs of soils used and their main properties. Characteristic diameters, uniformity coefficient (U), hydraulic conductivity (k), and density (ρ).

Photo	d_{10} (mm)	d_{60} (mm)	U (–)	k (m/s)	ρ (kg/L)
 Natural fluvial sand	0.11	0.31	2.82	$7.6 *10^{-7}$	1.69
 Soil A: 50 % gravel 2–5 mm + 50% fluvial sand	0.13	3.00	23.1	$1.2 *10^{-4}$	1.74
 Soil B: 50 % sand 0.2 mm + 50 % fluvial sand	0.12	0.28	2.3	$9.5 *10^{-6}$	1.66
 Soil C: 50 % crushed sand 0.5 mm + 50 % fluvial sand	0.1	0.39	4.1	$5.7 *10^{-5}$	1.61
 Soil D: 50 % sand 0.6 mm + 50 % fluvial sand	0.19	0.52	2.7	$2.2 *10^{-5}$	1.73

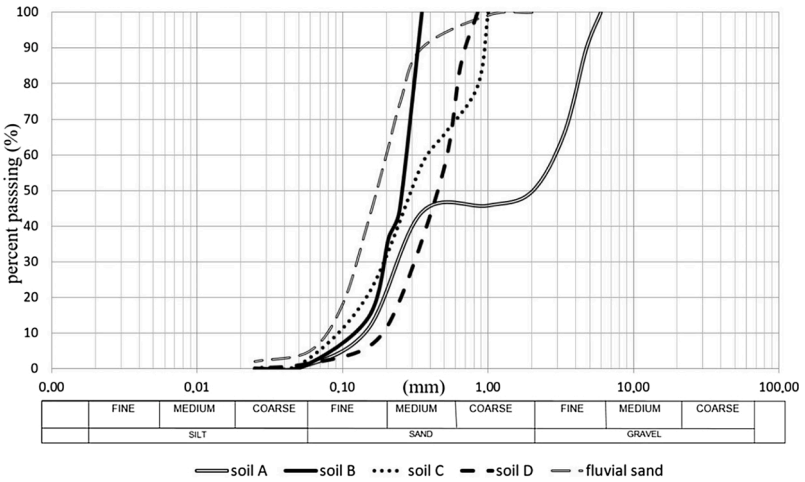

Fig. 2. Grain size distributions of soils used.

3. Tests and procedures performed

In the following paragraphs, the structure of the whole work is described. After the description of the research path, each test performed and its related procedures are explained.

3.1. Research path

First, a test campaign focused on the gel time was accomplished, whereupon the dynamic viscosity was also studied in depth. As briefly introduced before, the study of these two parameters was deemed fundamental from the viewpoint of the feasibly of a certain injection work. In fact, knowledge of them makes it possible, on one hand, to contribute to the best selection of the injection equipment (pumps, pipes etc.), and on the other, to control the operation in function of time, avoiding chocking of the system.

In the second phase, soil samples were grouted using accelerator dosages chosen to be suitable for a gelling time of about 15–60 min (the usual gelling time required on construction sites, as discussed by Chieregato, et al. [27]). Next, samples were cured for the programmed number of days and shaped in compliance with standard references and then tests were carried out. The mechanical characterization started with the assessment of the uniaxial compression strength (UCS). In the light of the UCS results, the subsequent test campaigns of tensile (Brazilian approach) and shear tests were performed using only acc1 (which showed better performance in terms of UCS).

3.2. Gelling time determination

The gel time (t_g) is a crucial parameter for a grouting operation performed by using colloidal nanosilica. It is defined as the time

Fig. 3. Rotational viscometer used (on the left) and spindle used (on the right). Spindle not to scale.

lapse between the mixing of colloidal nanosilica with accelerator and the loss of fluidity of the whole mixture [27]. From an operative point of view, it is the time span available for successfully carrying out a grouting operation with colloidal nanosilica, avoiding the block of pumps, chokings of injection lines or nozzles. Consequently, the assessment of the t_g should be the first step before to plan a grouting operation with colloidal nanosilica. Unfortunately, there is not a specific technical standard in the scientific literature that would allow operators to correctly and univocally assess the t_g. Consequently, a procedure similar to that introduced in Todaro et al. [32] for two-component grout was successfully applied: 0.2 l of colloidal nanosilica solution and the right amount of accelerator (in compliance with the testing dosage) were mixed by using a common laboratory mixer (rotation speed of 1800 rpm) for 10 s. After that, the product was gently poured from one tank to the other until the material was no longer able to flow. The frequency of pouring was not fixed but should be assessed in function of the forecasted t_g. Providing more details, considering that t_g is function of the type of accelerator and of its dosage, for forecasted gelling time shorter than 5 min, the frequency of pouring should be at least equal to once a second while for longer curing time also a frequency of once every 5 s is accepted. For curing time longer than 1 h, the frequency can be further increased. If there is no idea of the order of magnitude of t_g, the shorter frequency can be used (once a second).

3.3. Dynamic viscosity determination

Tests have been carried out according to A modality of ASTM D2196-18 [33]. It is reported that the prescription concerning the shaking and the curing of 1 h of the mixture before the dynamic viscosity assessment was not respected. This deviation from the standard regulation was due to the fast increasing of the dynamic viscosity. In fact, after the first contact between the nanosilica solution and accelerator the viscosity starts to grow almost instantaneously (especially for high accelerator dosages).

Pertaining to equipment, a rotational viscometer (model Alpha series, produced by Fungilab) was used (Fig. 3, left). The instrument was equipped with a spindle L1, (Fig. 3, right), that is, the one able to successfully recognize the lower values of viscosity. The spindle rotation speed was fixed equal to 100 rpm, kept constant for all the measurement. This choice intrinsically constrained the maximum value of the readable viscosity to 60 MPa*s (the maximum readable value for the chosen model of spindle and rotation speed, according to the viscometer software).

Different mixtures made up varying the volume percentages of colloidal nanosilica solutions and accelerator both were tested. A testing volume of 0.4 L was fixed. Beforehand, the proper amount of colloidal nanosilica solution and accelerator were prepared in two different tanks and after that the mixing occurs (the colloidal nanosilica solution has to be poured into the accelerator, in order to guarantee a suitable mixing). Immediately after mixing, the viscosity reading of the obtained mixture was initiated. Tests ended when the dynamic viscosity reached a value equal to 60 MPa*s. As the instrument was not equipped with an automatic system for reading/recording, outcomes were recorded manually.

3.4. Sample production

The sample production consisted of three phases: permeation grouting of the soils, curing of grouted samples under a protected environment (in moulds) and extraction of samples of grouted material.

The permeation grouting operation was performed by using procedures and equipment expressly designed for the purpose, modifying model schemes described in Kakavand and Dabiri [28] and Saiyouri et al. [11]. Before the grouting operation, as suggested in Saiyouri et al. [34] and Chupin et al. [35], the sample was completely saturated with water. The water was pumped with a pressure close to 20 bar, in order to compact the material intended for grouting. Fig. 4 depicts a simple scheme of the grouting arrangement.

The tank containing the liquid (water during the saturation/compaction phase and nanosilica + accelerator during the grouting phase) must be initially filled in order to simplify the insertion of the pump piston (roughly centrally in the tank). Prior to the grouting phase, colloidal nanosilica mixture was obtained by mixing sufficient quantities of nanosilica and accelerator for a duration of about 10 s by using a common laboratory mixer with a rotation speed of 1800. The pump (a one-component injection piston pump Taiver HTP 210,000 with a maximum pressure of 220–270 bar; Fig. 5) is connected to the sample mould with a high-pressure tube. Once the pump is activated, saturation/compaction phase runs until the water exits from the mould outlet hole. After that, the tank with water is

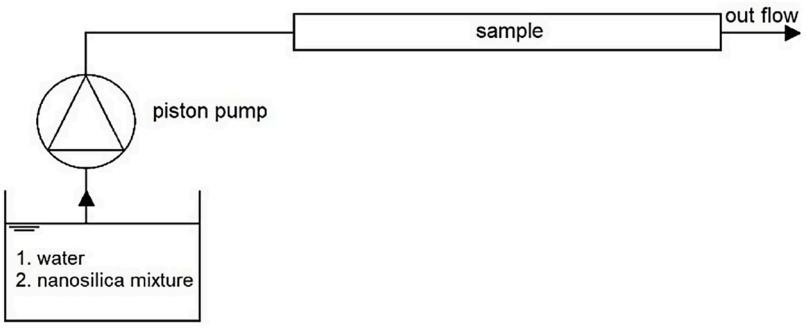

Fig. 4. Injection phase scheme. Water (1) is used during the saturation phase and then replaced by the nanosilica mixture (2) during the grouting phase.

Fig. 5. One-component injection piston pump Taiver HTP 210000 used for the sample grouting.

replaced by the tank with the colloidal nanosilica mixture, before long the grouting phase starts. This operation runs until the nanosilica mixture exits from the mould outlet hole. The nanosilica mixture is clearly recognizable from the white colour (Fig. 6, left). Only one mould can be grouted every cycle, and consequently it is strongly suggested that all mould patterns should be prepared in advance before starting the grouting.

The mould consisted of a PVC pipe, positioned horizontally during the grouting, with an external diameter of 63 mm, thickness of 5.5 mm, and length of 0.5 m (final sample diameter equal to 52 mm). Once the pump is activated, the liquid flows across the sample by exiting from the outlet hole located at the end of the circuit. The steps of the soil sample preparation are summarized in the following:

- A cylindrical mould (0.5 m long) is equipped at the edges with two specific threaded fittings, allowing the mould to be linked to connectors of smaller diameters (outlet and inlet connectors);
- The obtained mould has to be vertically positioned after previously tightening the outlet connector on one side;
- A layer of non-woven fabric must be carefully put inside the tube and located at the bottom. The layer must completely cover the circular inner section of the tube.
- A filter layer of 100 mm composed of gravel (medium grain size of 3 mm) is inserted and compacted by shaking the tube or dropping it from a height of less than 50 mm;
- The soil that should be grouted is inserted in the mould until the tube is completely filled. A gentle compacting action must be applied by shaking the tube or dropping it from a height of less than 50 mm;
- Eventually, the inlet connector is tightened, whereupon the connection with the pump can be accomplished.

The right hand part of Fig. 6 depicts a simplified scheme of the mould magnifying the tail in particular. On the left, images of the threaded fitting and outlet connector during the grouting phase are shown.

The pump pressure (up to 20 bar) serves for this purpose. The only drawback of this procedure consists in losing some centimetres of the samples due to the compaction action of the flow (detail in Fig. 7).

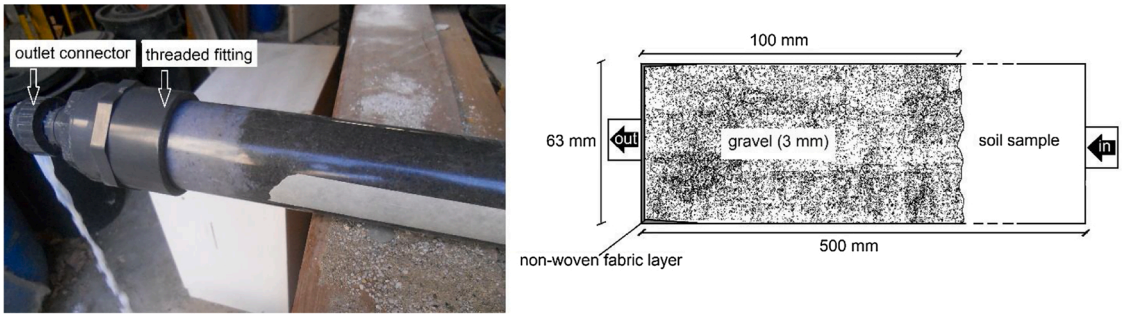

Fig. 6. Details of the sample tail. Left: photograph during the grouting phase. Right: a simple scheme (not to scale) of the filter system.

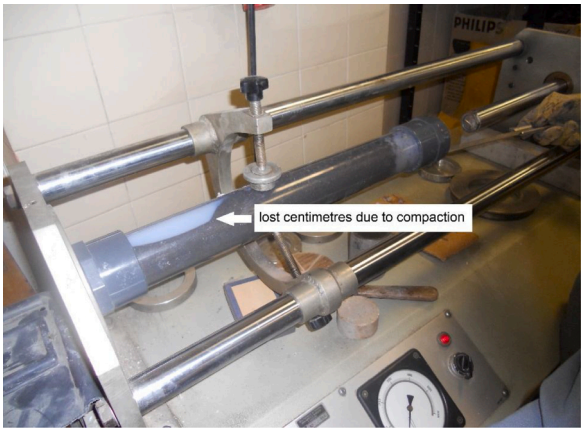

Fig. 7. Extraction phase. The lost sample centimetres due to the flow compaction action are clearly visible on the left of the picture.

Once the grouting phase has ended, the injected mould is conserved (the soil is inside the mould in a protected environment) in the laboratory (20 ± 2 °C) for 2 days. This phase is very important, since the grout gains the strength needed to avoid damage during extraction. After this time lapse, the extraction can be performed mechanically (Fig. 7). Eventually, samples are cured in the laboratory, always at the same controlled temperature. Samples are shaped immediately before testing according to the mentioned technical standards.

3.5. Uniaxial compression strength

The uniaxial compression strength was performed according to ASTM D7012-14 [36] method C. Concerning the standard suggestion of a stress rate between 0.5 and 1.0 MPa/s or a constant load speed for the whole test duration, the second choice was selected, respecting the constraint related to the test duration ranged between 2 and 15 min. Regarding the required sample dimensions of a length (h) to diameter (Φ) ratio of 2.0 or 2.5, this prescription was not respected; instead, samples with h/Φ equal to 1 were used. This reduction was necessary in order to maximize the number of samples obtained from a grouting-only operation, even though it was clear that the strength values assessed in this way were overestimated. However, if needed, a correction factor equal to 0.87 (ASTM C39/C39M-20 [37]) could be used in order to correct the imprecision related to the slimness factor. Tests were performed using a CONTROLS MX3 electro-hydraulic press. As for the samples shaping, cores obtained from the extraction phase were carefully notched for spans of 52 mm and cut by using a disc cutting machine. A tolerance on length of ±0.5 mm was accepted.

3.6. Indirect tensile strength

The indirect tensile strength (σ_t) was computed according to ASTM D3967-16 [38] (Brazilian test). The laboratory press used for the UCS test campaign was equipped with curved platens in order to better accommodate samples. It should be highlighted that also taking into account the minimum duration of the test equal to 1 min, the minimum loading rate of 0.05 MPa/s suggested by the regulation was found to be unusable. Consequently, the loading rate was strongly reduced and adapted (in function of the tested material) in order to respect the time constraint suggested by the technical reference. Averagely, the test duration was close to 4 min.

As for the samples shaping, cores obtained from the extraction phase were carefully notched for a thickness-to-diameter ratio (t/Φ) ranged between 0.2 and 0.75. The precision is not important and the cutting can be performed roughly, but always well within the range. On the contrary, the following step, namely the thickness measurement has to be performed accurately, since this dimension is needed for the computing of the tensile strength (Eq. 1). Once the peak force has been recorded (the load that generates a central crack able to split the sample in two parts), specifies computing the splitting tensile strength according to Eq. 1, which is valid for the Brazilian test carried out with curved platens:

$$\sigma_t = \frac{1.272\,P}{t\,\Phi\pi}\ (MPa) \tag{1}$$

where:

- P is the peak force (N)
- t is the sample thickness (mm)
- Φ is the sample diameter (mm).

3.7. Direct shear test

The direct shear tests were carried out according to EN ISO 17892-10:2018 [39]. As the samples were completely dry and stiff (after 14 days of curing, the nanosilica was completely crystallized), the porous discs were not used. Furthermore, considering the certainty of performing tests under drained condition (also confirmed by the absence of vertical displacement during the consolidation phase in preliminary tests), it was decided to set the duration of the consolidation phase at 15–20 s. The shear rate was set up equal to 5 mm/min. The vertical displacement was not recorded during the test. According to Lancellotta [40] 3 values of σ'_v are sufficient to identify a Mohr-Coulomb failure envelope criterion for a soil, however, for grouted material, a further higher value of σ'_v has been added, in order to increase the robustness of the analysis. The used vertical effective strengths (σ'_v) are reported in Table 3.

Differences between the vertical effective strengths are due to the different equipment used for the load application and for the different application surfaces in the case of soils without grouting (in this last case, a square Casagrande shear box was used instead of the cylindrical one).

4. Results and discussion

4.1. Determination of gelling time

Colloidal nanosilica A (CNA) and colloidal nanosilica B (CNB) were tested with both accelerators (acc1 and acc2). Starting from percentages by volume of 30 and 15 respectively, decreasing percentages were tested. The starting value of dosages were selected after a preliminary test campaign aimed at recognizing the meaningful testing ranges.

In Fig. 8, four functions describe the t_g trend in function of dosages. Dotted lines refer to CNB, while continue ones are related to CNA. In order to graphically distinguish accelerators, the triangle symbol is used for acc1 while the circle concerns acc2. It can be observed that functions related to the same accelerator are close. Consequently, it can be inferred that gel time is mainly affected by the kind of colloidal nanosilica rather than the kind of accelerator. It should however be remarked that functions related to acc2 are closer to each other respect the other couple. Furthermore, by fixing the type of colloidal nanosilica, it can be affirmed that a certain t_g could be reached by using acc2 with a lower dosage compared to acc1.

4.2. Dynamic viscosity determination

Figs. 9 and 10 report the viscosity trends related to acc1 and acc2, respectively. Independently of the type of nanosilica or accelerator, the functions describe invariably the same trend, which is easily comparable with the silica jellification trend [13]. Considering the CNA, two accelerator dosages were chosen: 20 and 25 % for acc1 and 7 and 8% for acc2. These dosages (by volume) were suggested by the supplier company's technicians. Once the dynamic viscosity trends had been assessed for CNA, the same tests were repeated using CNB. Tests were performed at a temperature of 15 °C.

The results show that CNB exhibited a gradient with higher growth than CNA even though the silica content of the mixture was lower. Considering Table 1, it can be speculated that fineness and a smaller particle size dimension have an influence on the viscosity trend. Taking into account both above figures, it can be noticed that while in Fig. 9 the first determinations (performed after 5 s) rapidly provide an idea of the viscosity trend (lower values correspond to a lower growth of viscosity), in Fig. 10 the outcomes are less clear, maybe due to a lower accuracy during testing. Finally and most importantly it can be stated that acc2 strongly boosts the gelling reaction.

4.3. Grouting test

All soils were successfully grouted. The pump pressure never exceeded 20 bars. The grouting mixtures were produced by using both accelerators according to the mixing procedure described above. The accelerator dosages were calibrated in order to obtain gelling times ranging between 15 and 60 min, according to Chieregato et al. [27]. Taking into account Fig. 8, the time lapse 15−60 min is detected on the order axis. After that, with horizontal projections on the experimental functions, 2 dosages can be spotted for each gelling time function. Anyway, considering that functions are basically flat for the referring time lapse, an average of dosages can be deemed meaningful for each couple of colloidal nanosilica and accelerator. Details concerning dosages are provided in Table 4.

Table 3
Vertical effective strengths for the direct shear tests.

σ'_v (kPa)		
CNA	CNB	No grouting
11.55	10.390	13.62
115.48	103.930	136.25
346.440	311.800	408.75
692.890	623.600	/

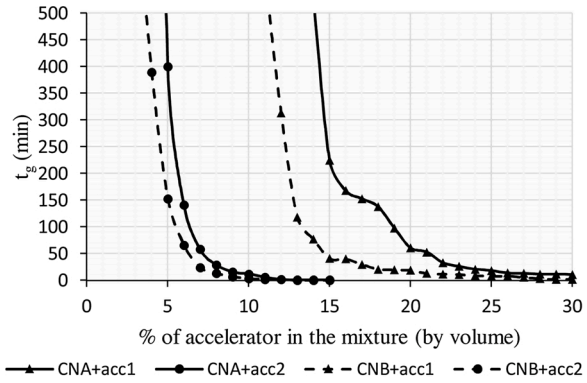

Fig. 8. Gelling time results.

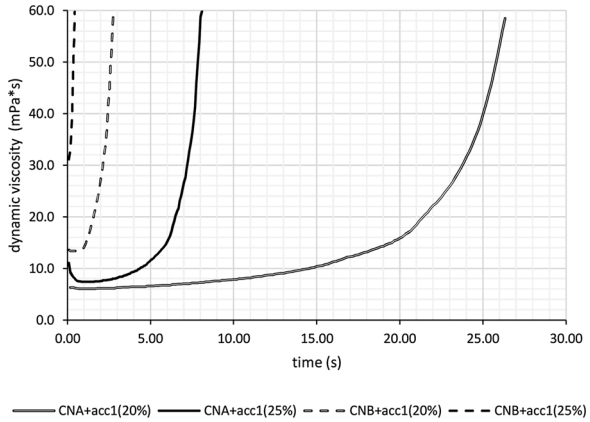

Fig. 9. Dynamic viscosity for accelerator 1. Dosages of 20 and 25 % by volume with respect to the nanosilica.

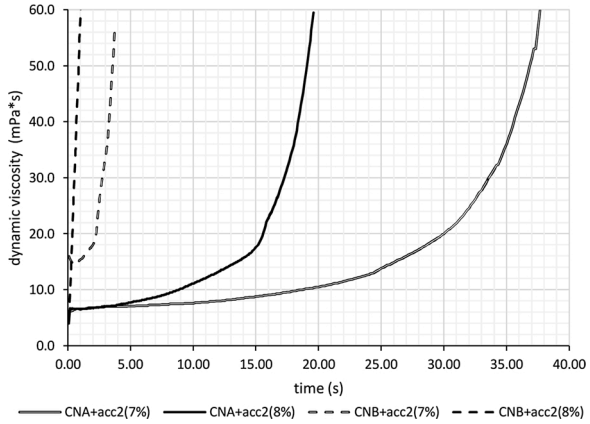

Fig. 10. Dynamic viscosity for accelerator 2. Dosages of 7 and 8% by volume with respect to the nanosilica.

4.4. Uniaxial compression test

Uniaxial compression tests were performed on samples obtained by grouting the four reference soils with CNA and CNB and the outcomes are reported in Fig. 11:on the top and on the bottom outcomes related to CNA and CNB are respectively reported. Moreover, on the left are showed data related to acc1, while ones related to acc2 are showed on the right. In labels, the following nomenclature has been used: kind of soil (with letter from A to D) + kind of colloidal nanosilica (CNA/CNB) + accelerator (acc1/acc2).

The curing time of 14 days was chosen as the time reference for the following analysis and discussion.

Table 4
Details of dosages used to achieve gelling times ranging between 15 and 60 min.

Mixture	Accelerator dosage (% by volume)
CNA + acc1	25 ± 2
CNA + acc2	8 ± 1
CNB + acc1	17 ± 3
CNB + acc2	7 ± 1

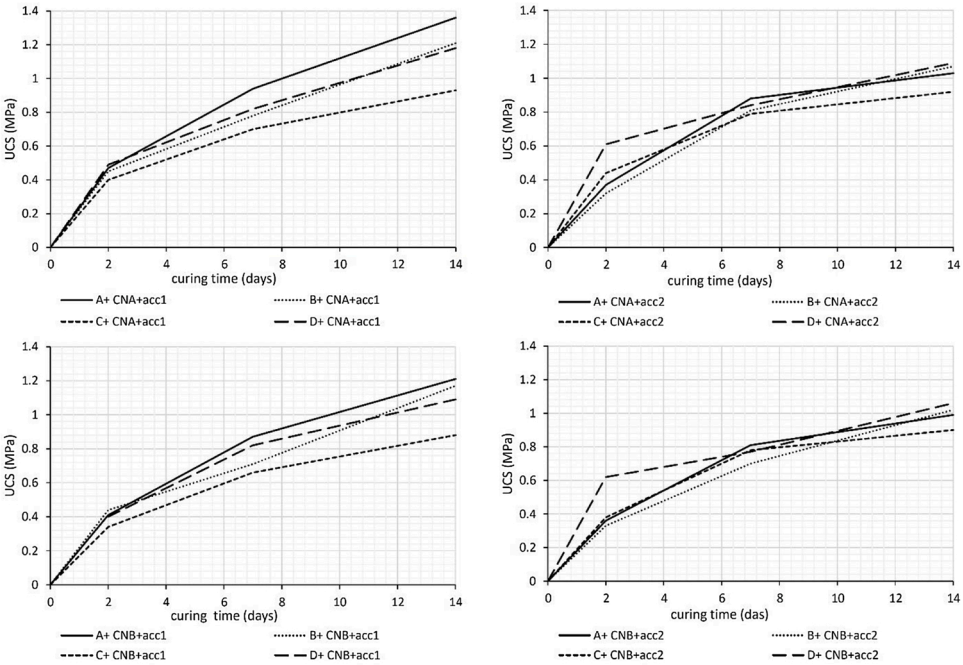

Fig. 11. UCS test campaign results. Labels follow the nomenclature: type of soil + type of nanosilica + type of accelerator.

Considering the results for CNA (Fig. 11, top), the values obtained by using acc1 are higher on average. Soil A seems to be more influenced by the different accelerators used, changing from a value close to 1.4 MPa for acc1 to about 1 MPa with acc2 respectively. Soils B and D are less influenced by the type of accelerator, with relative UCS increments of 13 and 8%, respectively, in the case of acc1. Soil C exhibited no variation. In CNB, (Fig. 11, bottom), the use of acc1 also led to higher UCS performances. The higher sensibility of soil A to the kind of accelerator was confirmed, with acc1 providing a UCS of almost 22 % higher than acc2. Soil B also exhibited an increment of the UCS (15 %) with acc1, while soils C and D seemed to be unaffected by the change of accelerator. The reason for the higher UCS performance obtained by using acc1 can be attributed to the lower concentration of NaCl, which permits strong nanosilica jellification due to the longer gelling time allowed compared to acc2 (Fig. 8). The high sensibility of soil A to the accelerator change and the contrasting insensibility shown by soil C surely depend on the grain size distribution although a specific test campaign should be performed expressly with the aim of investigating this aspect in more depth.

In order to highlight the effect of the kind of nanosilica, further consideration can be provided by fixing the type of accelerator; the

Table 5
Indirect tensile strength of samples grouted with CNA and CNB.

Soil + nanosilica	σ_t (kPa)
A + CNA	113.8
B + CNA	137.0
C + CNA	87.4
D + CNA	118.9
A + CNB	28.3
B + CNB	10.6
C + CNB	16.4
D + CNB	15.0

charts on the left in Fig. 11 can be compared, as can the charts on the right. Without exception, the outcomes highlight that CNA guarantees a higher UCS performance, with percentage increases of 3–12 % (depending on the soil) for acc1 and 2–5 % for acc2 (depending on the soil) with respect to the corresponding cases for CNB. In conclusion, taking into account the higher UCS results obtained by using acc1, this product was selected for the continuation of the mechanical characterization.

4.5. Indirect tensile test

Samples of soil grouted with both types of nanosilica and cured for 14 days were tested for indirect tensile strength (σ_t). The results are reported in Table 5.

The outcomes clearly highlight the higher tensile strength potentially obtained by using nanosilica A. It is interesting to notice that soil B was found to be the more sensible to the nanosilica variation ($\sigma_{t-CNA}/\sigma_{t-CNB}$ higher than 10), while Soils A and C were less sensible ($\sigma_{t-CNA}/\sigma_{t-CNB}$ close to 4–5).

4.6. Direct shear test

Samples of soil grouted with both types of nanosilica and cured for 14 days were tested. For each test campaign, natural soil (no grouting) and samples injected with both types of nanosilica were tested. The results were plotted on charts (τ–σ'_v) according to the Mohr-Coulomb failure criteria envelope, obtaining equations in the form $\tau = \alpha\,\sigma'_v + q$. Values of the cohesion c' (kPa) and friction angle φ' (°) were hence computed considering $c' = q$ and $\varphi' = \arctan(\alpha)$.

Fig. 12 summarizes all the shear tests carried out. The solid line refers to the soil grouted with CNA, the dashed one refers to the grouting performed using CNB, and the dotted one refers to the natural soil (no grouting). Unfortunately, concerning the soil D, the shear test related to the highest effective vertical strength was lost due to a mechanical problem occurred during the shearing phase. It was not possible to recover the peak value of the shear strength. Anyhow, according to Lancellotta [40], even with 3 points, the Mohr-Coulomb failure envelope criterion related to D + CNA can be considered reliable.

Fig. 13 reports the results in terms of cohesion (c') and friction angle (φ').

Taking into account the cohesion of natural soils, nanosilica A provided very high increments, with percentages ranging between 200 and 370 %. Soils injected with nanosilica B also exhibited growth in cohesion ranging between 50 and 90 %. It can be stated that soil A had the lower performance, with the lowest growth percentages (200 and 50 % for CNA and CNB respectively).

Considering instead the friction angle, analysis of the outcomes easily sheds light on how some tests on injected soils provided lower values than natural soils. In the specific case, for soil A and C this unexpected results were obtained. These outcomes were not considered as errors but, in the absence of experience and knowledge on the topic, helped the authors understand the sensibility of the test. In other words, the highest negative change equal to 7% computed considering the friction angle of the soil A + CNB and that of the natural soil A was established as the threshold for the critical analysis of the results. The occurrence of this phenomenon could be due to the highest values of uniformity coefficient and the presence of the bigger particles in soil A and B, respect other soils. Taking the limit of 7% as the significant variation percentage, it can be stated that for CNA only soils B and C exhibited growth of φ', with values of 22 and 16 % respectively. Considering CNB, only the friction angle of the soil B can be considered to have increased slightly, with an increment close to 9%.

5. Final remarks

According to Kakavand and Dabiri [28], grouting results confirm the ability of a nanosilica to successfully permeate different kind of sands characterized by a silt content close to 3%. The operation was performed with a pumping pressure lower than 20 bar on average independently of the nanosilica or accelerators used. The properties of the gel time and the viscosity, which are crucial for correct design of the grouting, cannot be generalized since they are extremely influenced by the types of both nanosilica and accelerator used. In more detail, it can be stated that the gel time and the viscosity trends are influenced by the accelerator dosage: by increasing it, the gel time can be reduced and the gradient of the growth in viscosity can be increased. Concerning accelerators, use of accelerator 2 guarantees that the required t_g can be obtained with a lower dosage with respect to accelerator 1. Hence, it can be stated that the higher the percentage of NaCl in the accelerator solution, the shorter t_g will be.

Taking into account the uniaxial compression test, it should be remarked that all tests were performed by using dosages in function of a fixed t_g equal to15–60 min. Generally speaking, after 14 days of curing, values of UCS close to 1 MPa, on average, were obtained. This result, in line with Chieregato et al. [27], exceeds values indicated in the scientific literature by Yonekura and Miwa [25] and Persoff et al. [26]. Analysing the obtained results by fixing the accelerator type, CNA exhibited higher performance. This result is believed to be due to the higher SiO_2 content. On fixing the type of nanosilica instead, accelerator 1 led to a higher UCS. Consequently, focusing on the final UCS result, it is suggested that a certain t_g can be reached by using a higher dosage of an accelerator deficient in NaCl rather than a smaller dosage of a product with a high NaCl concentration. Finally, it should be underlined that soil A, which was the coarser one, reached high values of UCS, confirming that the nanosilica can also be used satisfactorily in the case of sand characterized by a high percentage of gravel (50 % by weight).

Regarding the tensile strength, both nanosilica products were able to provide a certain degree of resistance versus tensile forces. Higher results exhibited by CNA were also confirmed in this case. Moreover, further details should be highlighted concerning the ratio UCS/σ_t: CNA exhibited an average value close to 10, while for CNB the results are more scattered but basically higher, ranging between 40 and 110. This discrepancy is due to the lower σ_t exhibited by CNB. These considerations underscored the higher sensibility of the

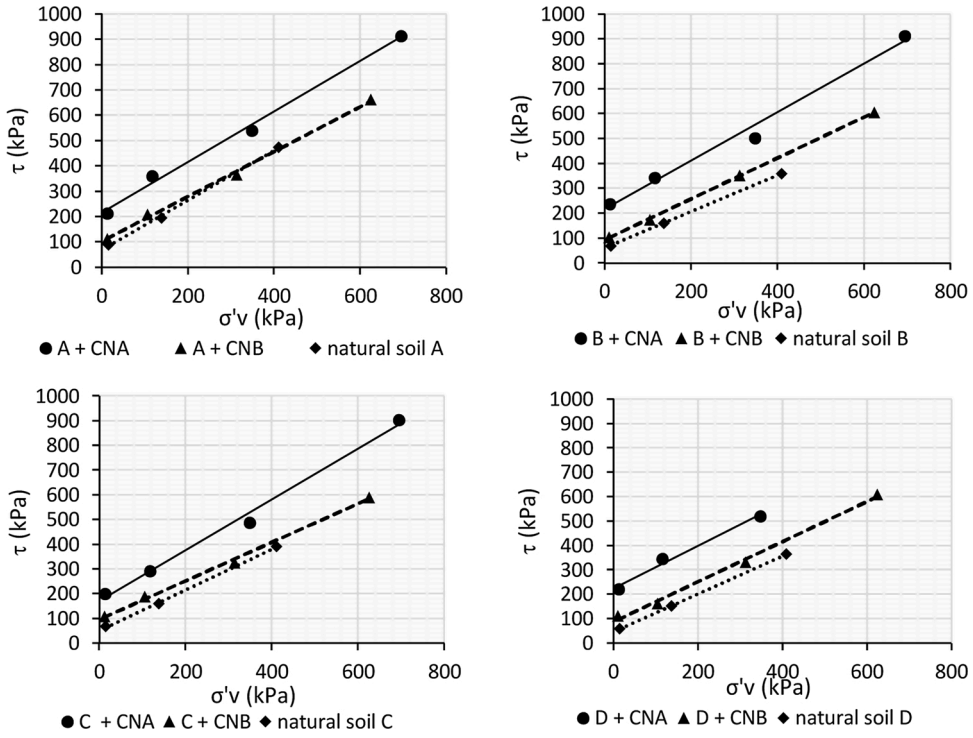

Fig. 12. Mohr-Coulomb failure criteria envelope concerning the four soils studied.

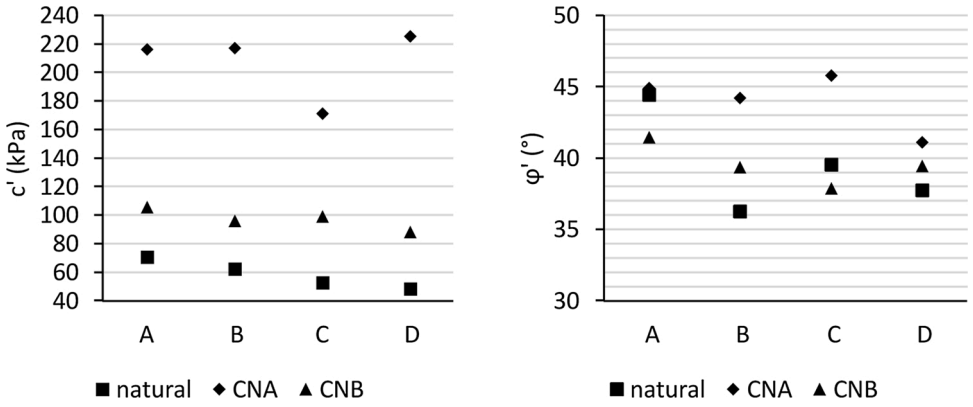

Fig. 13. Results of the shear test campaign in terms of cohesion (c') (left) and friction angle (φ') (right).

tensile strength to the change in the type of nanosilica with respect to the compression one.

In the shear tests, two different results were observed for c' and φ'. While marked increments could be observed for the cohesion independently of the colloidal nanosilica used, interpretation of the results of the friction angle was more difficult. With hindsight, vertical displacements during shearing could be useful for the interpretation of φ'. In conclusion, considering the precision of 7%, it can be stated that the grouting operation of the soil provided a clear and consistent increment of the friction angle only in the case of the fine and uniform ground (soil B). Finally, on comparing the obtained results with those described by Kakavand and Dabiri [28], the results did not overlap, since the increments were of a different order of magnitude for both cohesion and friction angle. This discrepancy, according to the authors' experiences, is believed to be due to the different colloidal nanosilica products used.

6. Conclusions

This research was planned and carried out with the purpose of filling the scientific gaps regarding the use of the colloidal nanosilica as material for grouting. The analysis of the scientific literature put alight the complete lack of researches focused on the colloidal nanosilica that, besides the study of the mechanical parameters of the grouted soils, provide also information on the nature of both the

nanosilica product and the accelerator. These aspects, namely knowing the SiO_2 percentage in the nanosilica solution and the NaCl concentration in accelerators, are crucial in order to correctly design a grouting operation, especially when the technical specification for a given construction site has to be satisfied. In fact, different results in terms of strength can be achieved by using different products.

This paper, according to the author knowledge, investigated in depth, for the first time, two main fundamental parameters of the system nanosilica-accelerator: the gelling time and the dynamic viscosity. The first parameter provide the available time lapse before the gelation of the mixture and it is useful for engineers for correctly organize the grouting phase without incurring drawbacks. The second parameter is mandatory for correctly choose the grouting equipment. As for the grouting phase, four different soils were prepared in laboratory and successfully grouted. After that, a complete mechanical characterization has been carried out and the order of magnitude of UCS, tensile strength and shear strength was provided. The author wants to highlight the outcomes of this preliminary research, despite being aware that further investigation is needed, also at the scale of the construction sites. However, the information provided could be of great interest to all the figures involved in grouting, undoubtedly useful for a preliminary design. Finally, it is important to underline that one product is not better than another, but designers should make the best choice for a grouting operation according to the final performance required.

Funding

This work is part of a PhD research developed in Politecnico of Turin, funded by BASF CONSTRUCTION CHEMICALS ITALIA.

Declaration of Competing Interest

The author report no declarations of interest.

Acknowledgements

The author wants to thanks BASF CONSTRUCTIONS CHEMICALS ITALIA for providing materials for the research. A special thanks to Dott. Davide Grassi and Dott. Franco D'Alessandro for technical suggestions and technical support during the experimental phase. Special thanks are owed to Prof. Daniele Peila for his suggestions.

References

[1] W. Chou, A. Bobet, Predictions of ground deformations in shallow tunnels in clay, Tunn. Undergr. Space Technol. 17 (1) (2002) 3–19, https://doi.org/10.1016/S0886-7798(01)00068-2.
[2] K.G. Holter, H.O. Hognestad, Modern pre-injection in underground construction with rapid-setting microcements and colloidal silica – applications in conventional and TBM-tunnelling, Geomech Tunn. 5 (2012) 49–56, https://doi.org/10.1002/geot.201200001.
[3] S.L. Shen, P.G. Atangana Njock, A. Zhou, H.M. Lyu, Dynamic prediction of jet grouted column diameter in soft soil using Bi-LSTM deep learning, Acta Geotech. 16 (2021) 303–315, https://doi.org/10.1007/s11440-020-01005-8.
[4] H.M. Lyu, S.L. Shen, Y.X. Wu, A.N. Zhou, Calculation of groundwater head distribution with a close barrier during excavation dewatering in confined aquifer, Geosci Front. 12 (2) (2021) 791–803, https://doi.org/10.1016/j.gsf.2020.08.002.
[5] S.L. Shen, H.M. Lyu, A. Zhou, L.H. Lu, G. Li, B.B. Hu, Automatic control of groundwater balance to combat dewatering during construction of a metro system, Autom Constr. 123 (2021) 103536, https://doi.org/10.1016/j.autcon.2020.103536.
[6] S.L. Shen, Z.F. Wang, J. Yang, C.E. Ho, Generalized approach for prediction of jet grout column diameter, J Geotech Geoenv Eng. 139 (12) (2013) 2060–2069, https://doi.org/10.1061/(ASCE)GT.1943-5606.0000932.
[7] Z.F. Wang, S.L. Shen, G. Modoni, A. Zhou, Excess pore water pressure caused by the installation of jet grouting columns in clay, Comput. Geotech. 125 (2020), 103667, https://doi.org/10.1016/j.compgeo.2020.103667.
[8] Z.F. Wang, S.L. Shen, G. Modoni, Enhancing discharge of spoil to mitigate disturbance induced by horizontal jet grouting in clayey soil: theoretical model and application, Comput. Geotech. 111 (2019) 222–228, https://doi.org/10.1016/j.compgeo.2019.03.012.
[9] K.G. Holter, E.D. Johansen, A. Hegrenaes, Tunnelling through a sandzone: ground treatment experiences from Bjoroy Subsea Road Tunnel, in: Proceedings of ITA WTC World Tunnel Congress North American Tunnelling, Washington DC (US), 1996. April.
[10] K. Garshol, Pre-injections in Tunnelling – A Useful Measure. Christian Veder Kolloquium, Injektionen in Boden Und Fels, Technical University Graz, Germany, 2002.
[11] N. Saiyouri, A.A. Alaiwa, P.Y. Hicher, Permeability and porosity improvement of grouted sand, Eur. J. Environ. Civil Eng. 15 (3) (2011) 313–333, https://doi.org/10.1080/19648189.2011.9693329.
[12] A. Chieregato, C.G. Oñate Salazar, C. Todaro, D. Peila, Mechanical improving of granular soils by permeation grouting: results of laboratory tests, in: Proceedings of ITA WTC World Tunnel Congress 2014 – Tunnels for a Better Life, Foz do Iguaçu (BR), 2021.
[13] H. Cambefort, The principals and applications of grouting, Q. J. Eng. Geol. Hydrogeol. 10 (1977) 57–95.
[14] E.B. Burwell, Cement and clay grouting of foundations: practice of the corps of engineering, J. Soil Mech. Found. Div. 84 (1) (1958) 1–22.
[15] M. Incecik, I. Ceren, Cement grouting model tests, Bull. Tech. Univ. Istanbul 48 (2) (1995) 305–317.
[16] A. Bodocsi, M.T. Bowers, Permeability of acrylate, urethane and silicate grouted sands with chemicals, J. Geotech. Eng. 117 (1991) 1227–1244.
[17] S. Akbulut, A. Saglamer, Estimating the groutability of granular soils: a new approach, Tunn. Undergr. Space Technol. 17 (4) (2002) 371–380, https://doi.org/10.1016/S0886-7798(02)00040-8.
[18] I.N. Markou, A.I. Droudakis, Factors affecting engineering properties of microfine cement grouted sands, Geotech. Geol. Eng. 31 (2013) 1041–1058, https://doi.org/10.1007/s10706-013-9631-9.
[19] M. Mollamahmutoğlu, Y. Yılmaz, I. Kutlu, Grouting performance of microfine cement and silica fume mix into sands, J. ASTM Int. 4 (4) (2007) 1–7, https://doi.org/10.1520/JAI100462.
[20] F. Kontoleontos, P.E. Tsakiridis, A. Marinos, V. Kaloidas, M. Katsioti, Influence of colloidal nanosilica on ultrafine cement hydration: physicochemical and microstructural characterization, Constr. Build. Mater. 35 (2012) 347–360.
[21] S. Zhang, W.-G. Qiaoa, P.-C. Chena, K. Xi, Rheological and mechanical properties of microfine-cement-based grouts mixed with microfine fly ash, colloidal nanosilica and superplasticizer, Constr. Build. Mater. 212 (2019) 10–18.
[22] S.C. Li, F. Sha, R.T. Liu, et al., Investigation on fundamental properties of microfine cement and cement-slag grouts, Constr. Build. Mater. 153 (2017) 965–974.

[23] S. Ferreiro, D. Herfort, J.S. Damtoft, Effect of raw clay type, fineness, water-to-cement ratio and fly ash addition on workability and strength performance of calcined clay-Limestone Portland cements, Cem. Concr. Res. 101 (2017) 1–12.
[24] J. Funehag, G. Gustafson, Design of grouting with silica sol in hard rock-new methods for calculation of penetration length, Part I, Tunn. Undergr. Space Technol. 23 (2008) 1–8.
[25] R. Yonekura, M. Miwa, Fundamental properties of sodium silicate based grout, in: Proceedings of 11th Southeast Asia Geotechnical Conference, Singapore, 1993, pp. 439–444.
[26] P. Persoff, G.J. Moridis, J.A. Apps, K. Pruess, Evaluation tests for colloidal silica for use in grouting applications, Geotech. Test J. 21 (1998) 264–269.
[27] A. Chieregato, C.G. Oñate Salazar, C. Todaro, D. Martinelli, D. Peila, Laboratory grouting test for waterproofing and consolidation of granular soils by means of innovative materials, Geoing Ambient Miner. 141 (1) (2014) 63–68.
[28] A. Kakavand, R. Dabiri, Experimental study of applying colloidal nano silica in improving sand-silt mixtures, Int. J. Nano Dimens. 9 (4) (2018) 357–373.
[29] C. Butrón, M. Axelsson, G. Gustafson, Silica sol for rock grouting: laboratory testing of strength, fracture behavior and hydraulic conductivity, Tunn. Undergr. Space Technol. 24 (2009) 603–607.
[30] G. Lazzara, S. Milioto, Dispersions of nanosilica in biocompatible copolymers, Polym. Degrad. Stab. 95 (4) (2010) 610–617, https://doi.org/10.1016/j.polymdegradstab.2009.12.007.
[31] ASTM, Standard Test Method for Permeability of Granular Soils (Constant Head). ASTM D2434-19, ASTM International, West Conshohocken (PA, USA), 2019.
[32] C. Todaro, L. Peila, A. Luciani, A. Carigi, D. Martinelli, A. Boscaro, Two component backfilling in shield tunneling: laboratory procedure and results of a test campaign, in: Proceedings of ITA WTC World Tunnel Congress, Naples (IT), 2019, pp. 3–9. May.
[33] ASTM, Standard Test Methods for Rheological Properties of Non-newtonian Materials by Rotational Viscometer. ASTM D2196-18, ASTM International, West Conshohocken (PA, USA), 2018.
[34] N. Saiyouri, M. Bouasker, A. Khelidj, Gas permeability measurement on injected soils with cement grout, Cem. Concr. Res. 38 (1) (2007) 95–103.
[35] O. Chupin, N. Saiyouri, P.Y. Hicher, The effects of filtration on the injection of cement based grouts in sand columns, Transp. Porous Media 72 (2007) 227–240.
[36] ASTM, Standard Test Methods for Compressive Strength and Elastic Moduli of Intact Rock Core Specimens Under Varying States of Stress and Temperatures. ASTM D7012:2014, ASTM International, West Conshohocken (PA, USA), 2014.
[37] ASTM, Standard Test Method for Compressive Strength of Cylindrical Concrete Specimens. ASTM C39/C39M-20, ASTM International, West Conshohocken (PA, USA), 2020.
[38] ASTM, Standard Test Method for Splitting Tensile Strength of Intact Rock Core Specimens. ASTM D3967-16, ASTM International, West Conshohocken (PA, USA), 2016.
[39] CEN ISO, Geotechnical Investigation and Testing – Laboratory Testing of Soil. Part 10: Direct Shear Tests. EN ISO 17892-10:2018, European Committee for Standardization, Bruxelles (B), 2018.
[40] R. Lancellotta, Geotecnica, Zanichelli, Bologna, 2001.